Enhancing Cancer Diagnosis: A Hybrid Level-Set and Edge Detection Approach for Accurate Medical Image Segmentation

Ismail Y. Maolood[1,2†]

[1]Department of Computer Science, College of Science, Knowledge University, Erbil 44001, Kurdistan Region – F.R. Iraq

[2]Department of Information and Communication Technology Center, Ministry of Higher Education and Scientific Research, Erbil, Kurdistan Region – F.R. Iraq

***Abstract*—Early diagnosis of cancer is crucial for improved patient results. With the aim of improving the effectiveness of cancer diagnosis, this paper introduces a new proposed method, computer-aided diagnosis, utilizing the level-set algorithm based on the edge detection approach for medical image segmentation. To assess the performance of our method, it was proved on a highly varied dataset that comprised liver cancer, Magnetic Resonance Imaging (MRI) brain cancer, and dermoscopy color images. By effectively integrating edge information into the level-set evolution process, the proposed method achieved impressive results. For liver cancer images, we obtained an accuracy of 0.9913, a sensitivity of 0.9165, and a Dice coefficient of 0.8820. Similarly, for dermoscopy color images, the method achieved an accuracy of 0.9979, a sensitivity of 0.9301, and a Dice coefficient of 0.9301. In the case of MRI images, the method demonstrated an accuracy of 0.9933, a sensitivity of 0.8591, and a Dice coefficient of 0.8591. The proposed method outperforms traditional techniques such as Simulated Annealing combined with Artificial Neural Network and Fuzzy Entropy with Level Set thresholding. This method demonstrates superior segmentation accuracy and robustness. By enabling precise identification of cancerous regions, this approach supports early diagnosis, reduces misdiagnosis, and enhances treatment planning, offering significant potential for improving cancer care and patient results.**

***Index Terms*—Cancer detection, Computer-aided diagnosis, Edge detection techniques, Level-set method, Medical image segmentation.**

I. Introduction

This Cancer remains one of the main causes of non-accidental death, so improving patients' survival requires accurate detection of the illness at an early stage (Al-Ayyoub, et al., 2015). Imaging is vital in cancer diagnosis and management as it gives the physician a picture of internal body structures that are vital in the detection and follow-up of malignant growths. However, it is a challenging process of image analysis, which must be done with special computer-aided tools to reveal carcinogens in non-cancerous tissues (Sharma, et al., 2013; Chan, Hadjiiski and Samala, 2020).

Osher and Sethian developed the Level-set method (LSM), a robust computational method widely utilized in cancer imaging to capture evolving shapes and interfaces (Osher and Sethian, 1988). LSM is particularly attractive to further segment complicated and asymmetrically formed cancers due to its topological modification. The aim of the proposed approach is to improve the technique for isolating malignant tissue by improving work with edge-detection algorithms. These techniques are applied for the identification of intensity fluctuations that may occur at the edges of a cancer picture. Edge detection methods, such as the Canny edge detector, help in the accurate outlining of the cancer edges with the help of large variations in an object's intensity (Canny, 1986; Kass, Witkin and Terzopoulos, 1988).

Computer-aided diagnosis (CAD) systems enhance the accuracy of medical image analysis, aiding radiologists and oncologists in diagnosing and treating various types of tumors (Sharma, et al., 2013; El-Baz, et al., 2013). These systems enable efficient analysis of large volumes of images, reducing the risk of human error. Accurate segmentation of tumors is crucial for treatment planning, as it provides information about their location, size, and extent. However, traditional segmentation methods, such as thresholding and region growing, often struggle to accurately delineate irregular tumor boundaries (Maolood, Al-Salhi and Lu, 2018b; Maolood, et al., 2018a; Halalli and Makandar, 2018).

The main aim of this study is to enhance the efficiency and accuracy of medical image segmentation for cancer diagnosis. The proposed CAD system combines the LSM algorithm with edge detection to achieve enhanced image segmentation and assessment. These systems would enhance the reliability of the segmentation details, sensitivity, and

ARO-The Scientific Journal of Koya University
Vol. XIII, No. 1 (2025), Article ID: ARO.11942 11 pages
DOI: 10.14500/aro.11942
Received: 12 December 2024; Accepted: 03 February 2025
Regular research paper; Published: 17 February 2025
†Corresponding author's e-mail: ismail.maulood@mhe-krg.org
Copyright © 2025 Ismail Y. Maolood. This is an open-access article distributed under the Creative Commons Attribution License (CC BY-NC-SA 4.0).

specificity and facilitate the early diagnosis and management of various types of cancer.

This project entails designing and evaluating a computer-aided diagnosis with level-set algorithm according to the edge detection technique (CAD-Ls-EDT) for contouring the cancerous regions in liver cancer, brain Magnetic Resonance Imaging (MRI), and dermoscopy color images. In this case, the aim is to improve the detection and separation of cancerous regions in those images using advanced computational techniques. The most important contribution of this investigation is to propose a solid and complete segmentation model to improve the identification and management of cancer, with the ultimate goal of providing oncology practitioners with the tools they need to carry out their work as successfully as possible.

The purpose of this study is to evaluate the effectiveness of a computer-aided diagnosis system based on a level-set algorithm and edge detection for the segmentation of medical images for the diagnosis of diseases, such as liver cancer, MRI, and dermoscopy images. Moreover, the proposed method enhances the level-set technique with edge detection, aiming to increase the segmentation accuracy of intricate and diverse cancerous tissues. This approach tries to address some of the issues of thresholding and region growth, which in segmentation, due to the complex and tricky shape of tumors (Maolood, Al-Salhi and Lu, 2018b; Kadhim, Khan and Mishra, 2022). The proposed methodology involves several sequential steps:

1. Preprocessing: The images are pre-processed, which is normalized for higher quality and removes any form of noise present with them. Usually, at this stage, Gaussian smoothing is applied.
2. Initial Contour Detection: An initial contour is established to direct the level-set evolution. Contouring is dependent on the image intensity gradients and edge information as the contour develops (Maolood, 2013).
3. Level-Set Evolution: The level-set formulation alters the contour of the cancer shape. This includes solving of partial differential equations (PDEs") as well as using gradient information of an image.
4. Edge Detection Integration: To enhance boundary detection, the level-set is implemented together with edge detection algorithms such as the canny edge detector. It helps to enhance the effectiveness of the segmentation results (Yin, et al., 2021).
5. Segmentation and Post-Processing: Finally, after contour modification to the appropriate shape, the final segmentation is grown. The morphological post-processing operation is also used to smooth the results of the segmented cancer image and to eliminate undesired structures (Maolood, Al-Salhi and Lu, 2018b).

CAD-Ls-EDT, which is discussed as the proposed approach that combines LSM and edge detection methods, proved to provide a high efficiency of cancer segmentation of various types. It is also knowledgeable that by incorporating the edge information in the LSM framework, the method was able to give correct margins around the cancers even in noisy and varying intensity levels. With CAD-L s-EDT, the high accuracy, sensitivity, and specificity were obtained as compared to conventional procedures. This advancement may have the potential to revolutionize practice in terms of diagnosis and treatment by offering the opportunity to identify abnormalities earlier and design the necessary treatment earlier.

The remaining research is prepared as follows: Section II contains part of the background. Section III gives the methodology. The finding of the study is presented in section IV. Finally, section V summarizes the investigation.

II. Background

A. Selecting Medical Image Segmentation

Medical image segmentation is the process of partitioning a cancer image into meaningful parts; usually, it has the goal of segmenting regions of interest, such as cancers (Maolood, Al-Salhi and Lu, 2018b). This very significant process aids in the detection and handling of several forms of cancers, such as liver cancer, brain cancer detected using MRI imaging, and skin cancers as deduced through the dermoscopy technique. Some of the traditional methods that are used to segment the cells include thresholding, region growing, and clustering, which can sometimes be very difficult because of the dynamic and complex nature of the malignant tissues.

It has great importance when it comes to liver cancer analysis because it helps draw boundaries between liver cancer and any cancers in CT or MRI scans. This also facilitates inaccurate assessment of the cancer size, position, and the stage of the disease, which is most important, especially when thinking of surgical or radiation therapy (Maolood, et al., 2018a; Halalli and Makandar, 2018). In MRI-based cancer diagnosis, the regions that should be targeted are the regions at which the cancer is located, and the process needs accurate segmentation. Segmentation provides higher degrees of accuracy in the regional characterization of disease, together with treatment planning and delivery, by better delineating between healthy and malignant tissues in vital organs, including the brain, breast, or prostate.

Segmenting the lesions from the skin in color images, dermoscopy practices image segmentation in the identification of skin cancer. It contributes to increasing the understanding of Accelerator people with the Lesion morphological aspect that contributes to the identification of melanoma as well as other skin cancers at an early stage of development. These segmentation techniques not only help in the diagnosis of diseases but also help in the efficiency and effectiveness of treatment plans using higher mathematics and artificial intelligence (Kadhim, Khan and Mishra, 2022; Aziz and Abdulla, 2023; Maolood, 2013; Jaganathan and Kuppuchamy, 2013).

B. Cancer Analysis Based on a Level-set Method

LSM, which was introduced by Osher and Sethian in 1988, is a well-suited computational method used in the modeling of the evolution of shapes and interfaces. In the area of medical image segmentation, LSM is especially suitable for the definition of intricate patterns that are also in constant

change, such as tumors (Osher and Sethian, 1988). According to LSM, the changing envelopment is the zero-level-set of a higher-dimensional function that represents the advanced complex interface, which can track topological changes and detailed shapes. This makes it useful for partitioning different forms of cancer with complex margins and different signal strengths.

The radiological images that might be used in the medical diagnosis could be in grayscale or color. Let Y = (X.Y) represents the coordinates of all pixels in the medical image within the cancerous region, while I = (x, y) denotes the specific pixel coordinates within the cancer region being analyzed. It is dynamic, with the level-set function being tested at a certain position m(t) and time t yielding a value of 0 (Aziz, et al., 2023). This may be important in dealing with problems at the uppermost layers or frontiers of Equation (1).

$$\varnothing\,(m(t).\,t) = 0 \tag{1}$$

When dealing with partial differential equations (PDEs) and level-set method, the function ∅ (t.x.y) usually means the level-set function (Hemanth, Anitha and Balas, 2015; Friedrich, et al., 2016). This function is defined in the spatial domain (x.y) at a particular time t. The level-set function experiences time changes, and it is true that the zero level-set is the boundary of the chosen malignancy. As is depicted in Fig. 1, this explains Equation (2).

$$m(t)=\begin{cases} \varnothing\,(t.x.y)<0\,(x.y) \text{ is inside } m(t) \\ \varnothing\,(t.x.y)=0\,(x.y) \text{is at } m(t) \\ \varnothing\,(t.x.y)>0\,(x.y) \text{is outside } m(t) \end{cases} \tag{2}$$

Information on a curved surface is influenced by multiple factors from both external and internal research archives. In medical imaging, regions of interest, such as cancerous areas, can be defined using a level-set function ∅ (t.x.y) < 0, which represents the tumor boundary m(t)at time t. The function classifies points as follows: ∅ (t.x.y) < 0 for points inside the cancerous region, ∅ (t.x.y) = 0 for points on the tumor boundary, and ∅ (t.x.y) > 0 for points outside the cancerous region.

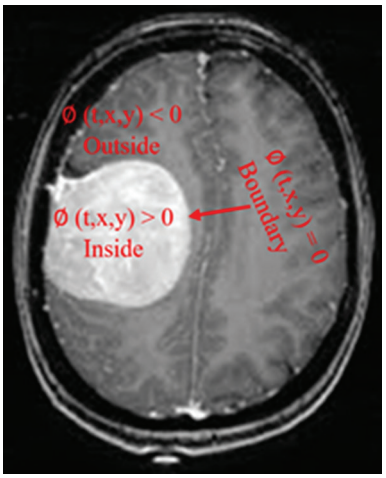

Fig. 1. Normal direction curve propagation of LSM.

As mentioned from equation (3), which describes the dynamics of a boundary of cancerous, where ∅t = 0 represents the cancer boundary. The symbol $\frac{\partial \varnothing}{\partial m(t)}$ transforms the chain rule, which helps in seeing how ∅ grows in response to time, while x_t represents the velocity field that dictates the motion of the boundary cancer.

$$\frac{\partial \varnothing}{\partial m(t)}\,xt + \varnothing t = 0 \tag{3}$$

Use the normal component of $\frac{\partial \varnothing}{\partial m(t)}$ | to find the desired velocity on the interface *xt*, (4) becomes.

$$\begin{cases} \frac{\partial \varnothing}{\partial t} + f\left|\nabla \varnothing\right| = 0 \\ \varnothing(0.x.y) = \varnothing_0\,(x.y) \end{cases} \tag{4}$$

While |∇∅| is the gradient magnitude, which indicates the natural direction to the boundary. The term $\frac{\partial \varnothing}{\partial t}$ is the time evolution of ∅, and ∅(0.x.y)=$\varnothing_0$ (x.y) is the initial condition for the cancer boundary (Chan and Vese, 2001; Chen, et al., 2002). To stop level-set growth at the perfect solution, regularize using an edge indication function *g*. A popular level-set segmentation method is.

$$g = \frac{1}{1+\left|\nabla\left(G_\sigma * I\right)\right|^2} \tag{5}$$

The convolution of the medical image is represented by G_σ * I. With Gaussian noise G^σ, ∇ the process for the cancer image gradient is denoted by ∇, and a function g exhibits minimal variation around within the specified boundaries (Maolood, Al-Salhi and Lu, 2018b). An often-utilized formulation for level-set segmentation is.

$$\frac{\partial \varnothing}{\partial \varnothing} = \left|\nabla \varnothing\right|\left(\operatorname{div}\left(\frac{\nabla \varnothing}{\left|\nabla \varnothing\right|}\right)\right) \tag{6}$$

The gradient magnitude |∇∅| ensures that the motion is normal to the cancer boundary, while the term $\left(\operatorname{div}\frac{\nabla \varnothing}{\left|\nabla \varnothing\right|}\right)$ represents the curvature of the boundary. This curvature flow drives the boundary to reduce high-curvature regions, leading to a smoother shape. The cancer image quality has been enhanced with the use of computer-aided diagnosis utilizing the level-set algorithm based on the edge detection approach (CAD-Ls-EDT).

C. Medical Image Analysis for Cancer Boundary Detection

Cancer boundary detection is a critical field of study and advancement in medical image analysis. In medical imaging, the process entails using complex algorithms and methodologies to precisely detect and demarcate the borders of cancerous

http://dx.doi.org/10.14500/aro.11942

areas, including liver cancer, MRI cancers, and dermoscopy color images. Precise cancer border identification is critical for diagnosing, planning therapy, and monitoring cancer patients (Bechar, et al., 2024; Khaliki and Başarslan, 2024).

Cancer boundary detection is undergoing rapid advancements, with researchers consistently striving to enhance the accuracy and efficiency of algorithms (Mercaldo, et al., 2023; Hosseini, Monsefi and Shadroo, 2024). It has the potential to make the diagnosis and treatment planning of cancer more effective and favorable for the patients. However, it is vital that algorithms are used as such to assist decision-making instead of as tools to replace the medical profession. Healthcare professionals should always retain the finality of choices relating to diagnosis and treatment decisions (Suryawanshi and Patil, 2024).

Cancer segmentation is among the initial steps applied to the medical image, and therefore, edge detection forms the core of the medical image examination task. Edge detection enhances the definition of the boundaries of tumors and anatomical structures, hence the location of rigorous intensity transformation. This information may then be utilized to enhance the segmentation algorithms to yield better results (Zhu, et al., 2024; Shao, et al., 2024).

The Canny Edge Detector, as put forth by John F. Canny in 1986, has been one of the prevailing practices employed in edge detection for computers. However, it is most valuable as a method for finding edges in intensity in medical imaging, where changes in intensity are often indicative of the cancer or other structures' boundaries (Yang, et al., 2024). Here are some of the steps for cancer segmentation:

Step 1: Apply the Gauss smoothing filter before edge detection to reduce the amount of cancer image noise, which can help focus on prominent features for cancer analysis (Badar, et al., 2024).

$$G(x.y) = \frac{1}{2\mu\sigma^2} e^{\frac{x^2+y^2}{2\sigma^2}} \tag{7}$$

Where: G (x.y) Value of the Gaussian function at the pixel (x.y), σ: Standard deviation of the Gaussian distribution.

Step 2: Calculate the magnitude and direction of the gradient of cancer images using four angles (0, 45, 90,135 degrees) by solving equations (8) and (9).

$$G = \sqrt{G_x^2 + G_y^2} \tag{8}$$

$$G\theta = \arctan\left(\frac{G_y}{G_x}\right) \tag{9}$$

Where G_x and G_y a direction according to x and y.

Step 3: Non-maximum suppression removes non-edge pixels on the cancer image, leaving only well lines.

Step 4: Select a hysteresis threshold by utilizing two thresholds to determine which edges to include or exclude.

Step 4.1: Strong Edge Pixels: Pixels with a gradient magnitude overhead the high threshold (T_h) are classified as robust edge pixels.

Step 4.2: Weak Edge Pixels: Pixels with a gradient magnitude under the high threshold (T_h) are repressed.

Step 4.3: Edge Linking: Pixels with a gradient magnitude among the low and high thresholds (T_h and T_l) are considered weak edge pixels. These pixels are reserved only if they are connected to a strong edge pixel through several weak edge pixels. This helps to ensure that the detected edges are continuous and well-defined. Where (T_h) determines the minimum gradient magnitude to classify a pixel as a strong edge and (T_l) helps identify weak edges that are potentially part of true edges but need validation.

In this research, we recommend a new technique that integrates LSM with edge detection approaches to enhance the efficiency and reliability of cancer segmentation. Incorporating the edge information into the level-set evolution process, our method aims to overcome the drawbacks of existing conventional methods and aims to provide enhanced and efficient segmentation results that help in achieving better clinical results.

III. Methodology

A. Data Acquisition

A variety of datasets that used liver cancer images, MRI scans, and dermoscopy color images were used. All the images used in this study were obtained from the open-access database available through MIRA – McMaster Institute for Research on Aging (Maolood, Al-Salhi and Lu, 2018b). Some datasets contain images with confirmed cancer diagnoses; thus, the experimental results were credible.

A total of 620 images were employed for this study, where 200 of which were liver cancer images, 260 of which were brain MRI images, and 160 of which were dermoscopy color images. This diverse dataset contained images of small to large cancer sizes.

The proposed methodology comprises three distinct phases. Initially, we assess the efficacy, competence, and precision of our approach by comparing it with three other regularly utilized procedures for the segmentation of medical images. Another step displays the efficacy of our approach. Ultimately, the third phase involves the implementation and evaluation of the suggested technique for segmenting cancer images.

The techniques were implemented in MATLAB R2022b (MathWorks) on a Windows 11 Home version 22H2 machine with a 64-bit operating system, an ×64-based processor, an Intel Core i7-8550U CPU @ 1.80 GHz, and 16 GB of RAM. Our technology has the possibility to suggestively improve the accuracy and efficiency of cancer detection using medical image segmentation.

All images were pre-processed to enhance image quality and reduce noise. Pre-processing steps included:

- Noise Reduction: Gaussian filtering was applied to remove noise and improve image clarity.
- Intensity Normalization: Images were normalized to a common intensity range to ensure consistent pixel values.

The pre-processed dataset was utilized to train and evaluate the proposed CAD-Ls-EDT method.

B. Proposed Method

Scientists have devised cancer image segmentation techniques for addressing cancer issues. The suggested method aims to improve computer-aided diagnosis by utilizing a level-set algorithm along with an edge detection method to accurately find and separate images of cancerous borders. The objective is to generate valuable data on the limits of cancer and effectively categorize cancer cases. The research employs a variety of techniques to provide efficient segmentation, as seen in Fig. 2.

Below is our proposed algorithm for computer-aided diagnosis with a level-set algorithm according to the edge detection technique.

Algorithm 1: CAD-Ls-EDT cancer image segmentation

```
Input: Cancer image.
Output: extracted the cancerous part and then segmented it
Create a loop for reading the medical image with initial boundaries of cancer region
for x in range(medical_image.shape[0]):
 for y in range(medical_image.shape[1]):
 if ϕ [x, y] > 0: # Process as inside the cancer part
 process_inside (ϕ, x, y)
 elif ϕ [x, y] == 0: # Process as boundary of the cancer part
 process_boundary (ϕ, x, y) # Process as outside the cancer part
 else:
 process_outside (ϕ, x, y)
def double_threshold(cancer_image, low_thresh, high_thresh):
 output = np.zeros_like(cancer_image, dtype=np.uint8)
 strong_edges = (cancer_image >= high_thresh) # Strong edges
 output[strong_edges] = 255
 weak_edges = (cancer_image >= low_thresh) & (image < high_thresh) # Weak edges
 output[weak_edges] = 128 # Mark weak edges with a distinct intensity
return output extracted the cancer part
```

Our proposed algorithm is explained systematically for each step.

Input: Cancer image.

Output: extracted the cancerous part and then segmented it.

Step 1: Cancer Image Input and Initialization

Load the input cancer image into the system. Create an initial level-set function ϕ (x,y,t) to represent the initial contour. This contour should enclose the approximate region of interest. Define the parameters for the level-set evolution process, such as the time step, stopping criteria, and edge detection thresholds.

Step 2: Check for Valid Input

Ensure that the input image is valid and meets the required format and size specifications. If the cardinality of the set ∅ (t.x.y) is greater than zero, then proceed to enter the cancer image. If the set of points ∅ in the coordinates (t.x.y) is equal to zero, then proceed to the edge of the cancer image. If ∅ (t.x.y) < 0, then go outside of the cancer image, according to Eq. (2).

Step 3: Level-Set Evolution

Compute the gradient of the image to obtain information about intensity changes. Evolve the level-set function using the mathematical explanation of the level-set equation (Eq. 3). This involves iteratively updating the level-set function based on the image gradients and the current contour position. Monitor the modification in the level-set function between iterations. If the change is below a pre-defined threshold, the iteration process is terminated.

Step 4: Edge Detection and Refinement

If the function g is near zero in a boundary of the cancer by Eq. (5) and go to Eq. (6) to select the part of cancer segmentation.

Step 5: Thresholding

Use two thresholds (T_h and T_l), to classify edge pixels. Pixels with a gradient magnitude above T_h are classified as robust edge pixels, while those below T_l are repressed. Pixels with a gradient magnitude between (T_h and T_l) are measured weak edge pixels. Weak edge pixels are connected to robust edge pixels to form continuous edge segments.

Step 6: Extract and Segment Cancerous Region

Use the final level-set function to extract the segmented region, which corresponds to the area enclosed by the zero-level-set (following Eq. 9). Apply post-processing methods, such as morphological processes, to perfect the segmentation results and remove any small artifacts or noise. Display the original image, the initial contour, the final segmentation result, and any relevant metrics (e.g., Dice coefficient, Jaccard index).

Step 7: Iteration and Termination

If the level-set function has converged or a maximum number of iterations has been reached, terminate the algorithm. If the level-set function has not converged, return to Step 3 and continue the evolution process.

Step 8: End

IV. Results And Discussion

A. Experimental Step

The effectiveness of the proposed CAD-Ls-EDT method was tested in experiments on a benchmark dataset of medical images. These were liver cancer images, brain MRI images, and dermoscopy color images, which have been sourced from different places. It was meant to compare this method and its effectiveness in segmenting cancerous areas in images of different levels of complexity and noise added to them.

The results of the experiment show that the performance of the suggested CAD-Ls-EDT method depends on certain

http://dx.doi.org/10.14500/aro.11942

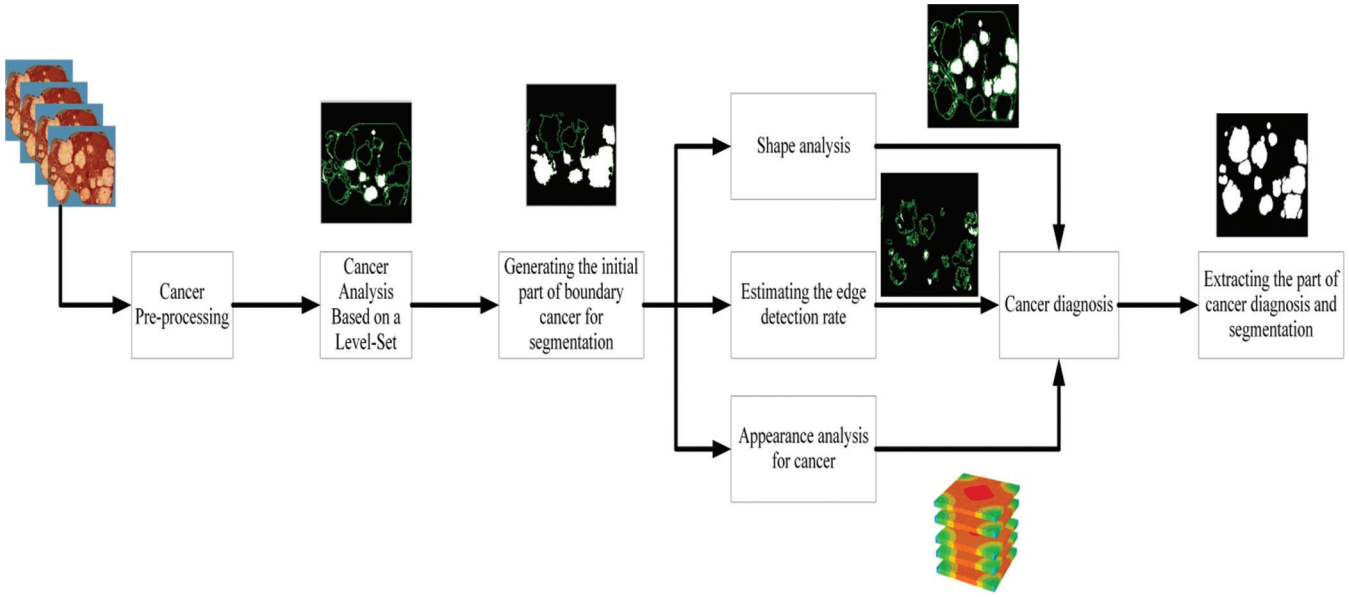

Fig. 2. Presents a computer-aided diagnosis system that selects and extracts high-quality boundary cancer images for diagnosis and segmentation.

features of the input image data. The method effectively applies image segmentation techniques to arrange noise in medical images while enhancing the image quality to enhance successive segmentation techniques. The study employs a computer-aided diagnosis system based on a level-set method and edge detection to ensure high-quality segmenting boundaries of cancer in images.

The first experimentation of the CAD-Ls-EDT algorithm shown in Fig. 3 involves a liver image with sizes of 620 × 620 pixels. Column (a) shows the original image with cancer, and in column (b), we use a circular initial counter with λ parameters ranging from $\lambda 1 = 1$ to $\lambda 2 = 8$, $\mu = 0.31$, and a maximum number of iterations of 80 to find the boundary of the cancer within the image. The segmentation result in our proposed technique is represented in column (c), established after optimizing the parameters to yield the finest outer border of cancer on the image. Specifically, we set the λ parameter to 4, μ to 0.6, and performed 30 iterations.

Fig. 4 illustrates the segmentation results for a dermoscopy color image with dimensions of 650 × 650 pixels. The original image is shown in column (a). An initial circular contour was defined with parameters $\lambda 1 = 1$, $\lambda 2 = 8$, and $\mu = 0.3$, and the level-set method was iterated 80 times to search for the cancer boundary. The optimal segmentation result, shown in column (c), was obtained by adjusting the parameters to $\lambda 1 = 3$, $\lambda 2 = 4$, $\mu = 0.2$, and 45 iterations. These parameter settings effectively delineated the cancer boundary, demonstrating the ability of the proposed method to accurately segment complex regions in dermoscopy images.

Fig. 5 illustrates the segmentation results for a 512 × 512 pixel MRI image. Column (a) shows the original MRI image containing a cancerous region. An initial circular contour was defined with parameters $\lambda 1 = 1$, $\lambda 2 = 8$, and $\mu = 0.3$, and the level-set method was iterated 80 times to search for the cancer boundary. The optimal segmentation result, shown in column (c), was obtained by adjusting the parameters to $\lambda 1 = 4$, $\lambda 2 = 6$, $\mu = 0.4$, and 25 iterations. These parameter settings effectively delineated the cancer boundary, demonstrating the ability of the proposed method to exactly segment complex regions in MRI images.

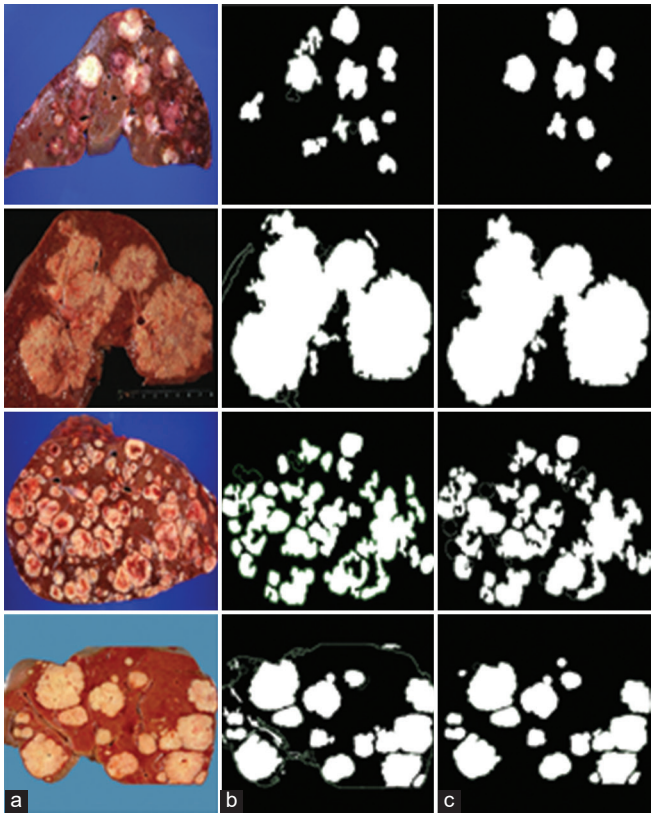

Fig. 3. Computer-aided diagnosis using the level-set method with edge detection (a) The original liver image with cancer; (b) the search for the cancer's boundary region; and (c) the segmentation of the cancer after 30 iterations and extracting the cancer region.

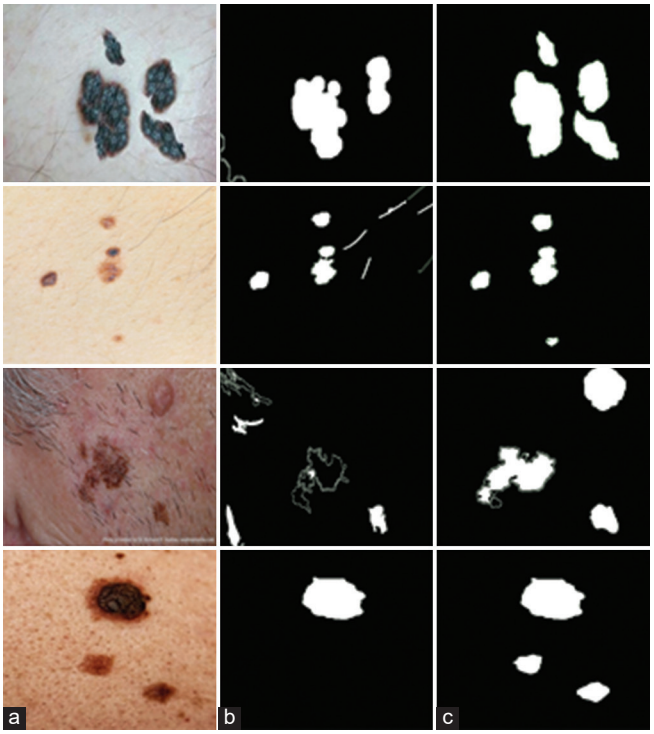

Fig. 4. Computer-aided diagnosis with the level-set method by using edge detection: (a) original dermoscopy color image; (b) searching to find the boundary region of cancer; (c) finding the cancer and segmenting after 45 iterations by extracting the cancer region.

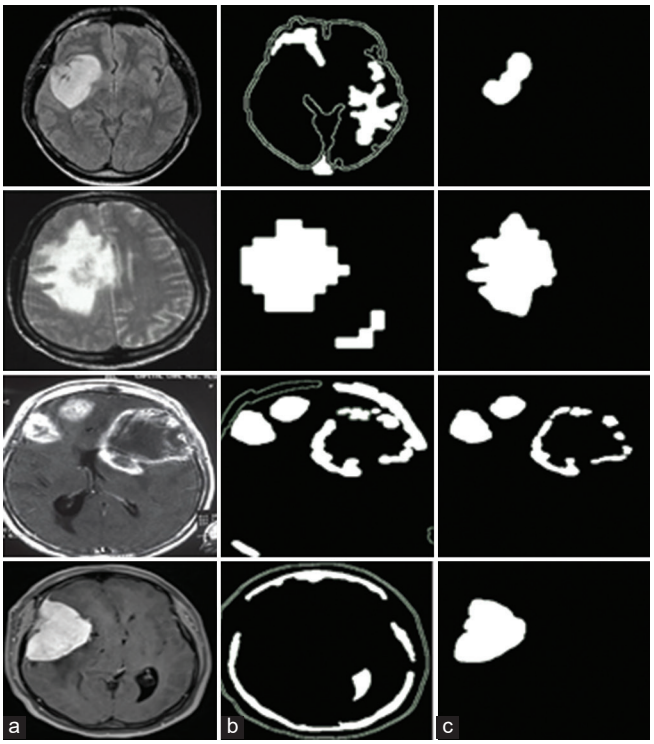

Fig. 5. Computer-aided diagnosis with the level-set method by using edge detection: (a) original image; (b) searching to find the boundary region of cancer; (c) finding the cancer and segmenting after 25 iterations by extracting the cancer region.

B. Experimental Results

To assess the CAD-Ls-EDT approach proposed in this paper, experiments were performed on a dataset including liver cancer, skin cancer, and MRI cancer images. For liver cancer images, an initial circular contour was defined with parameters $\lambda 1 = 1$, $\lambda 2 = 8$, and $\mu = 0.31$. The level-set method was then repeated (80 times) to enhance the contour and obtain the best parameters for segmentation. By trying the proposed framework on several images, it was possible to find the correct values of the parameters under consideration for each type of image. The same optimal values of $\lambda 1 = 2$, $\lambda 2 = 4$, $\mu = 0.6$, were established for preliminary enhancement of liver cancer images, with 30 iterations. Similarly, for dermoscopy color images, optimal parameters were found to be $\lambda 1 = 3$, $\lambda 2 = 4$, $\mu = 0.2$, and 45 iterations. In the case of MRI images, the optimal parameter settings were $\lambda 1 = 4$, $\lambda 2 = 6$, $\mu = 0.4$, and 25 iterations. These optimized parameter values were useful in defining the cancer regions with high levels of accuracy for all the different types of images.

Evaluation of the proposed CAD-Ls-EDT method is based on the assessment of the segmented cancer area obtained with the hybrid technique concerning to cancer segmentation (CS) ground truth (GT) data provided by the clinicians. These coefficients are very important for processes to measure the similarity between the ground truth and the cancer-segmented region, known as the Jaccard Coefficient and Dice Coefficient, both these values range from zero to one, where higher values are for an accurate segmentation of cancer. Among them, the Jaccard coefficient is more suitable for this research because of the potential partial overlaps and complexity in cancer boundaries (Maolood, et al., 2018a). In addition, efficiency criteria, including sensitivity, reveal the primary features of cancers. Precision is the degree of correctness of the approximate quality of cancer parts, specificity they can exclude non-cancer parts, and accuracy are some of the key measures that determine how successfully the proposed hybrid level-set and edge detection technique can detect non-cancerous and cancer parts. The level-set and edge detection approach distinguish between non-cancerous and cancerous parts. Taken together, the above parameters are evidence of the effectiveness of the hybrid algorithm in successfully attaining reliable segmentation, which is critical for enhancing the accuracy of cancer diagnosis and optimization of treatment planning (Maolood, Al-Salhi and Lu, 2018b). The parameter metrics details are providing mathematically as trails:

$$\text{Similarity of } Jaccard\ Coefficient = \frac{|GT \cap CS|}{|GT \cup CS|} \tag{10}$$

$$\text{Similarity of } Dice\ Coefficient = \frac{2 * |GT \cap CS|}{|GT| + |CS|} \tag{11}$$

http://dx.doi.org/10.14500/aro.11942

$$\text{Performance of Sensitivity} = \frac{TP}{TP + FN} \quad (12)$$

$$\text{Performance of Precision} = \frac{TP}{TP + FP} \quad (13)$$

$$\text{Performance of Specificity} = \frac{TN}{TN + FP} \quad (14)$$

$$\text{Performance of Accuracy} = \frac{TP + TN}{TP + TN + FP + FN} \quad (15)$$

$$\text{Matthews Correlation Coefficient}(\text{MCC}) = \frac{(TP * TN) - (FP * FN)}{\sqrt{(TP + FP) * (TP + FN) * (TN + FP) * (TN + FN)}} \quad (16)$$

Where

- True Positive (TP): Correctly segmented cancer regions.
- False Positive (FP): Non-cancer regions incorrectly identified as cancer.
- True Negative (TN): Non-cancer regions correctly identified as non_cancer.
- False Negative (FN): Cancer regions missed by the segmentation.

As shown in Table I and Fig. 6, the performance of the proposed CAD-Ls-EDT algorithm was assessed on the discussed metrics of accuracy, precision, sensitivity, specificity, Matthews's correlation coefficient, Dice coefficient, and Jaccard index. When evaluated using the liver cancer images, the method attained an accuracy of 0.9913, a precision of 0.7538, a sensitivity of 0.9165, an MCC of 0.8630, a Dice coefficient of 0.8820, and a Jaccard index of 0.8650.

In dermoscopy color images, the proposed method provided an accuracy of 0.9979, an average precision of 0.8956, a sensitivity of 0.9301, an MCC of 0.9317; a Dice coefficient of 0.9301, and a Jaccard index of 0.8705. The values of accuracy, precision, sensitivity, MCC, Dice, and Jaccard coefficients were produced as 0.9933, 0.8437, 0.8591, 0.8936, 0.8591, and 0.7687 for MRI images, respectively. These results also show the efficiency of the proposed method in the segmentation of the different classes of cancer images.

The CAD-Ls-EDT method presented high performance with all the image types where high accuracy, sensitivity, and specificity were obtained. The excellent values achieved by the method concerning the Dice coefficient, MCC, and the Jaccard index demonstrate the ability to define the cancer margins and the differentiation between cancerous and non-cancerous tissues. These results provide sufficient evidence to suggest that the CAD-Ls-EDT method is a useful technique for cancer diagnosis and treatment planning.

Therefore, the results of the current experiments support the improvements of the suggested CAD-Ls-EDT method

TABLE I
HIGH-QUALITY MEDICAL SEGMENTATION IS REQUIRED FOR THE DETECTION OF CANCER IMAGES

Medical test	Liver image	Dermoscopy image	MRI image
Accuracy	0.9913	0.9979	0.9933
Precision	0.7538	0.8956	0.8437
Sensitivity	0.9165	0.9301	0.8591
MCC	0.8630	0.9317	0.8936
Dice coefficient	0.8820	0.9301	0.8591
Jaccard Coefficient	0.8650	0.8705	0.7687
Specificity	0.9910	0.9862	0.9930

MRI: Magnetic Resonance Imaging

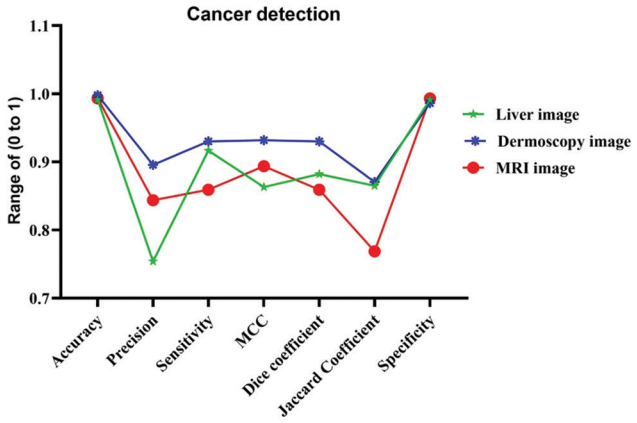

Fig. 6. Performance evaluation of computer-aided diagnosis with the level-set method by using edge detection method in cancer detection across different medical imaging modalities.

for medical segmentation and cancer detection. Given that the described method has high accuracy, sensitivity, and specificity about different types of images, it can be used for cancer diagnostics at an early stage and further treatment planning. The generalized evaluation runs several performance measures to confirm the standardized method's effectiveness and precision, which is far superior to classic segmentation techniques. This situates CAD-Ls-EDT as a move forward in the categorization of cancer images with positive potential for shaping the clinical histories of cancer patients.

C. Comparison with the New Traditional Methods

The proposed method, called CAD-Ls-EDT, which combines the level-set approach and edge detection techniques, outperforms conventional segregation techniques. As presented in Table II, the proposed method improves the sensitivity, specificity, and precision of various cancer images, such as liver cancer images, dermoscopy color images, and MRI images. For instance, in liver cancer images, CAD-Ls-EDT achieves a sensitivity of 0.9165 and an accuracy of 0.9913, significantly outperforming methods, such as Simulated Annealing combined with Artificial Neural Network (SA-ANN) and Fuzzy Entropy with Level Set (FELs) thresholding, which have sensitivities of 0.88 and 0.83, for accuracy of 0.97 and 0.98, respectively(Maolood, Al-Salhi and Lu, 2018b; Win, et al., 2018).

This higher performance can be explained by the incorporation of edge detection with a level-set method that leads to better boundary delineation and segmentation. The CAD-Ls-EDT method, when supplemented with edge detection, can provide more accurate and noise-resistant segmentation for complex shapes of cancers as compared to the present methods of segmentation.

Fig. 7 presents the segmentation results of the proposed CAD-Ls-EDT and the typical approaches. It also contains the evaluation of both methods. The figure also demonstrates that the proposed method offers better specificity, sensitivity, accuracy, and precision compared to the other. According to the results, the CAD-Ls-EDT method is the most sensitive using MRI cancer images, with a comfort level of sensitivity score of 0.8591. The above example demonstrates how efficient the method is in determining true positives and is very imperative in early diagnosis.

Similarly, for dermoscopy color images, the sensitivity that is achieved with 0.9301 is quite higher than that received from several approaches out of them, FLog Parzen Level-set (FPLS) (Virupakshappa, Veerashetty and Ambika, 2022) and SA-ANN (Win, et al., 2018). This clearly shows that the overall performance of the CAD-Ls-EDT method is better in terms of detecting true positive images in dermoscopy images. As for the assessment of the specificity, it is also very high in the case of the CAD-Ls-EDT method. The specificity scores in the case of liver cancer, dermoscopy color cancer, and MRI cancer images are 0.9910, 0.9862, and 0.9930, respectively. These high specificity values indicate the method's ability to correctly recognize true negative cases, reducing the risk of false positives and unnecessary treatments.

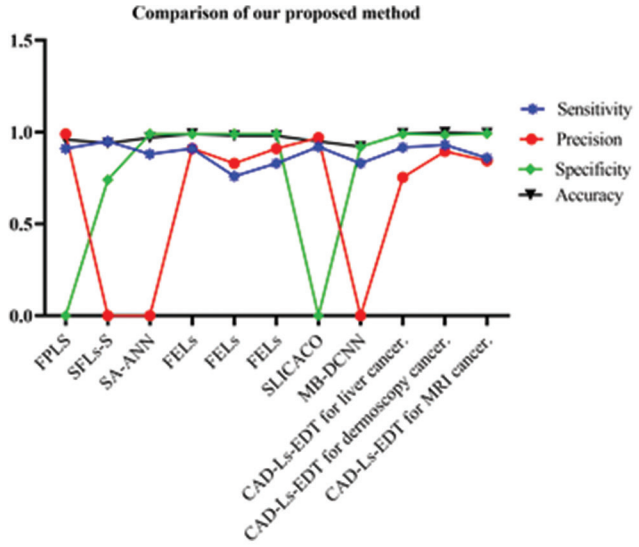

Fig. 7. Detailed comparison of our proposed method with current standard techniques.

The accuracy of positive predictions, or known as precision, is also quite high in our proposed method. The results of the precision score for the dermoscopy color image are 0.8956. It is slightly higher at 0.9910 for liver and MRI cancer and 0.9930; however, these scores are comparatively higher than other methods. Higher precision of the method in the identification of liver and MRI cancer points toward correct identification, and hence, the ability to reduce false positives is very high.

In addition, from Table III, it is noticeable that the proposed CAD-Ls-EDT method demonstrates excellent performance in the overlap measurements, including the Jaccard index and Dice coefficient, which are valuable measures of the quality of the segmentation. In the case of liver cancer, skin cancer, and MRI cancer images, we get a Dice coefficient of 0.8820, 0.9301, and 0.8591, A Jaccard Index of 0.8650, 0.8705, and 0.7687, respectively, which shows a high similarity between the segmented area and ground truth. The above-established performance is considerably better than other improved methods, such as the GAPBFCM and the MB-DCNN, whose Dice coefficients and Jaccard ratios are significantly lower (Latha and Perumal, 2020; Pei, et al., 2017).

Incorporation of the edge information into the LSM framework improves contour development, hence improving the results in image segmentation. This makes the CAD-Ls-EDT method suitable for early cancer detection and for planning the most suitable procedure.

TABLE II
Compare Our Suggested Method (Cad-Ls-Edt) to the Newest Research on Quality Cancer Segmentation Using Sensitivity, Specificity, Precision, and Accuracy as the Criteria for Evaluation

Compare Algorithm	Sensitivity	Precision	Specificity	Accuracy
FLog Parzen Level Set (FPLS) (Virupakshappa, Veerashetty and Ambika, 2022)	0.91	0.99	Non	0.96
Simulated annealing combined with an artificial neural network (SA-ANN) (Win, et al., 2018)	0.88	Non	0.99	0.97
Fuzzy entropy with a level set (FELs) thresholding for Ultrasound Image (Maolood, Al-Salhi and Lu, 2018b)	0.91	0.91	0.99	0.99
Fuzzy entropy with a level set (FELs) thresholding for MRI Image (Maolood, Al-Salhi and Lu, 2018b)	0.76	0.83	0.99	0.98
Fuzzy entropy with a level set (FELs) thresholding for MRI Image (Maolood, Al-Salhi and Lu, 2018b)	0.83	0.91	0.99	0.98
Simple linear iterative clustering (SLIC) and ant colony optimization (ACO) algorithms (SLICACO) (Singh, Janghel and Sahu, 2021)	0.92	0.97	Non	0.95
MB-DCNN (Xie, et al., 2020)	0.83	Non	0.92	0.92
Our proposed method (CAD-Ls-EDT) for liver cancer image	0.9165	0.7538	0.9910	0.9913
Our proposed method (CAD-Ls-EDT) for dermoscopy color cancer	0.9301	0.8956	0.9862	0.9979
Our proposed method (CAD-Ls-EDT) for MRI cancer	0.8591	0.8437	0.9930	0.9933

CAD-Ls-EDT: Computer-aided diagnosis with level-set algorithm according to edge detection technique

TABLE III
COMPARISON OF OUR PROPOSED METHOD (CAD-LS-EDT) WITH THE LATEST STUDIES ON QUALITY CANCER SEGMENTATION, TAKING INTO ACCOUNT THE JACCARD INDEX AND DICE COEFFICIENT AS THE CRITERIA FOR EVALUATION

Compare Algorithm	Dice Coefficient	Jaccard index
Genetic algorithm probability based Fuzzy C-Means (GAPBFCM) (Latha and Perumal, 2020)	0.91	0.91
Novel density-based fuzzy c-mean algorithm (D-FCM) (Pei, et al., 2017)	0.89	0.80
Fuzzy entropy with a level set (FELs) thresholding for Ultrasound Image (Maolood, Al-Salhi and Lu, 2018b)	0.91	0.92
Fuzzy entropy with a level set (FELs) thresholding for MRI Image (Maolood, Al-Salhi and Lu, 2018b)	0.79	0.97
MB-DCNN (Xie, et al., 2020)	0.90	0.82
Fuzzy entropy with a level set (FELs) thresholding for Dermoscopy Image (Maolood, Al-Salhi and Lu, 2018b)	0.87	0.95
Simple linear iterative clustering (SLIC) and ant colony optimization (ACO) algorithms (SLICACO) (Singh, Janghel and Sahu, 2021)	0.91	0.84
Our proposed method (CAD-Ls-EDT) for liver cancer image	0.8820	0.8650
Our proposed method (CAD-Ls-EDT) for dermoscopy color cancer	0.9301	0.8705
Our proposed method (CAD-Ls-EDT) for MRI cancer	0.8591	0.7687

CAD-Ls-EDT: Computer-aided diagnosis with level-set algorithm according to edge detection technique

V. CONCLUSION

The proposed (CAD-Ls-EDT) approach, which combines edge detection techniques with the level-set method from medical image segmentation, has been tested and found to detect various forms of cancer. It has specific applications in increasing the accuracy, sensitivity, and specificity of the detected cancer in images, which include liver cancer, brain MRI, and dermoscopy color images.

Enhancing boundary detection, the proposed CAD-Ls-EDT method provides better boundaries around the cancer regions than most segmentation methods. This is the enhanced segment, which plays a critical role in the diagnosis of the diseases and the initial management of the diseases, and the segment, which makes the patient lives.

The experimental results have shown that the application of the CAD-Ls-EDT methodology results in high values of the important performance indicators, such as true positive rate, Jaccard, MCC, and Dice coefficients. These measures contribute to the efficiency level and correctness of the method for medical image analysis.

Similarly, the CAD-Ls-EDT method will also be very useful for oncologists and radiologists to enhance the segmentation quality of the medical images with high accuracy to obtain accurate diagnostic data. This enhancement in the computer-aided diagnostic approach is a profound leap in the war against cancer, particularly in achieving enhanced clinical prognosis because of early and accurate diagnosis and therapies.

REFERENCES

Al-Ayyoub, M., Abu-Dalo, A.M., Jararweh, Y., Jarrah, M., and Sa'd, M.A., 2015. A GPU-based implementations of the fuzzy C-means algorithms for medical image segmentation. *The Journal of Supercomputing,* 71, pp.3149-3162.

Aziz, M.H., and Abdulla, A.A. 2023. Computer-aided diagnosis for the early breast cancer detection. *UHD Journal of Science and Technology*, 7, pp.7-14.

Aziz, S.A., Hawbani, A., Wang, X., Abdelhamid, T., Maolood, I.Y., Alsamhi, S., and Ismail, A., 2023. *Improving Brain MRI Image Segmentation Quality: A Hybrid Technique for Intensity Inhomogeneity Correction. In: 34th Conference of Open Innovations Association (FRUCT)*. IEEE, United States, pp.20-26.

Badar, T., Särkkä, S., Zhao, Z., and Visala, A., 2024. Rao-blackwellized particle filter using noise adaptive kalman filter for fully mixing state-space models. *IEEE Transactions on Aerospace and Electronic Systems*, 60, pp.6972-6982.

Bechar, A., Elmir, Y., Himeur, Y., Medjoudj, R., and Amira, A., 2024. *Federated and Transfer Learning for Cancer Detection Based on Image Analysis*. [arXiv preprint arXiv:2405.20126].

Canny, J., 1986. A computational approach to edge detection. *IEEE Transactions on Pattern Analysis and Machine Intelligence*, 8, pp.679-698.

Chan, H.P., Hadjiiski, L.M., and Samala, R.K., 2020. Computer-aided diagnosis in the era of deep learning. *Medical Physics,* 47, pp.e218-e227.

Chan, T.F., and Vese, L.A., 2001. Active contours without edges. *IEEE Transactions on image Processing*, 10, pp.266-277.

Chen, Y., Tagare, H.D., Thiruvenkadam, S., Huang, F., Wilson, D., Gopinath, K.S., Briggs, R.W., and Geiser, E.A. 2002. Using prior shapes in geometric active contours in a variational framework. *International Journal of Computer Vision*, 50, pp.315-328.

Elizângela, D.S.R., Fátima, N.S.DM., Regis, C.P.M., Chagas, J.V.S., Guimarães, M.T., Santos, L.O., Medeiros, A.G., and Peixoto, S.A, 2021. Level set approach based on Parzen Window and floor of log for edge computing object segmentation in digital images. *Applied Soft Computing*, 105, p.107273.

El-Baz, A., Beache, G.M., Gimel' Farb, G., Suzuki, K., Okada, K., Elnakib, A., Soliman, A., and Abdollahi, B., 2013. Computer-aided diagnosis systems for lung cancer: Challenges and methodologies. *International Journal of Biomedical Imaging*, 2013, p.942353.

Friedrich, T., Kötzing, T., Krejca, M.S., and Sutton, A.M., 2016. The compact genetic algorithm is efficient under extreme gaussian noise. *IEEE Transactions on Evolutionary Computation*, 21, pp.477-490.

Halalli, B., and Makandar, A., 2018. Computer aided diagnosis-medical image analysis techniques. *Breast Imaging*, 85, p.109.

Hemanth, D.J., Anitha, J., and Balas, V.E., 2015. Performance improved modified Fuzzy C-Means algorithm for image segmentation applications. *Informatica*, 26, pp.635-648.

Hosseini, S.H., Monsefi, R., and Shadroo, S., 2024. Deep learning applications for lung cancer diagnosis: A systematic review. *Multimedia Tools and Applications,* 83, pp.14305-14335.

Jaganathan, P., and Kuppuchamy, R., 2013. A threshold fuzzy entropy based feature selection for medical database classification. *Computers in Biology and Medicine*, 43, pp.2222-2229.

Kadhim, Y.A., Khan, M.U., and Mishra, A., 2022. Deep learning-based computer-aided diagnosis (cad): Applications for medical image datasets. *Sensors* (*Basel*), 22, p.8999.

Kass, M., Witkin, A., and Terzopoulos, D., 1988. Snakes: Active contour models. *International Journal of Computer Vision*, 1, pp.321-331.

Khaliki, M.Z., and Başarslan, M.S., 2024. Brain tumor detection from images and comparison with transfer learning methods and 3-layer CNN. *Scientific Reports*, 14, p.2664.

Latha, C., and Perumal, D., 2020. Segmentation of brain tumour MR images in soft computing techniques. *Journal of Theoretical and Applied Information Technology*, 98, p.3164-3171.

Latha, C., and Perumal, K., 2020. Brain tumour segmentation using genetic and ant colony. *International Journal of Advanced Research in Engineering and Technology*, 11, pp.1643-1654.

Maolood, I.Y., 2013. *Fuzzy C-means Clustering Algorithm with Level Set for MRI Cerebral Tissue Segmentation.* Universiti Teknologi Malaysia, Malaysia.

Maolood, I.Y., Al-Salhi, Y.E.A., Alresheedi, S., Ince, M., Li, T., and Lu, S.F., 2018a. *Fuzzy C-Means Thresholding for a Brain MRI Image Based on Edge Detection. In: 2018 IEEE 4th International Conference on Computer and Communications (ICCC)*. IEEE, pp.1562-1566.

Maolood, I.Y., Al-Salhi, Y.E.A., and Lu, S., 2018b. Thresholding for medical image segmentation for cancer using fuzzy entropy with level set algorithm. *Open Medicine*, 13, pp.374-383.

Mercaldo, F., Brunese, L., Martinelli, F., Santone, A., and Cesarelli, M., 2023. Object detection for brain cancer detection and localization. *Applied Sciences*, 13, pp.9158.

Osher, S., and Sethian, J.A., 1988. Fronts propagating with curvature-dependent speed: Algorithms based on Hamilton-Jacobi formulations. *Journal of Computational Physics*, 79, pp. 12-49.

Pei, H.X., Zheng, Z.R., Wang, C., Li, C.N., and Shao, Y.H., 2017. D-FCM: Density based fuzzy c-means clustering algorithm with application in medical image segmentation. *Procedia Computer Science*, 122, pp.407-414.

Shao, J., Luan, S., Ding, Y., Xue, X., Zhu, B., and Wei, W., 2024. Attention connect network for liver tumor segmentation from CT and MRI images. *Technology in Cancer Research and Treatment,* 23, p.1-11.

Sharma, P., Malik, S., Sehgal, S., and Pruthi, J., 2013. Computer aided diagnosis based on medical image processing and artificial intelligence methods. *International Journal of Information and Computation Technology*, 3, pp.887-892.

Singh, L., Janghel, R.R., and Sahu, S.P., 2021. SLICACO: An automated novel hybrid approach for dermatoscopic melanocytic skin lesion segmentation. *International Journal of Imaging Systems and Technology,* 31, pp.1817-1833.

Suryawanshi, S., and Patil, S.B., 2024. Brain tumor detection using YoloV5 and faster RCNN. *International Journal of Intelligent Systems and Applications in Engineering*, 12, pp.335-342.

Virupakshappa, S., Veerashetty, S., and Ambika, N., 2022. Computer-aided diagnosis applied to MRI images of brain tumor using spatial fuzzy level set and ANN classifier. *Scalable Computing: Practice and Experience*, 23, pp.233-249.

Win, K.Y., Choomchuay, S., Hamamoto, K., Raveesunthornkiat, M., Rangsirattanakul, L., and Pongsawat, S., 2018. Computer aided diagnosis system for detection of cancer cells on cytological pleural effusion images. *BioMed Research International*, 2018, p.6456724.

Xie, Y., Zhang, J., Xia, Y., and Shen, C., 2020. A mutual bootstrapping model for automated skin lesion segmentation and classification. *IEEE Transactions on Medical Imaging*, 39, pp.2482-2493.

Yang, W., Chen, X.D., Wang, H., and Mao, X., 2024. Edge detection using multi-scale closest neighbor operator and grid partition. *The Visual Computer*, 40, pp.1947-1964.

Yin, J., Chang, H., Wang, D., Li, H., and Yin, A., 2021. Fuzzy C-means clustering algorithm-based magnetic resonance imaging image segmentation for analyzing the effect of Edaravone on the vascular endothelial function in patients with acute cerebral infarction. *Contrast Media* and *Molecular Imaging*, 2021, p.4080305.

Zhu, Z., Sun, M., Qi, G., Li, Y., Gao, X., and Liu, Y., 2024. Sparse dynamic volume TransUNet with multi-level edge fusion for brain tumor segmentation. *Computers in Biology and Medicine*, 172, p.108284.